Synthesis and Characterization of Partially Metallic Chromium Hollow Nanospheres: A Step toward the Tuning of Magnetic Property

[1]Hafiz Rub Nawaz*, [1]Barkat Ali Solangi, [1]Kashif Pervez, [1]Farman Ahmed and [2]Hongbin Cao
[1]*Leather Research Centre PCSIR D-102 South Avenue SITE Area Karachi Pakistan.*
[2]*Institute of Process Engineering CAS Beijing 100080 China.*
nawazhr@yahoo.com*

(Received on 10th December 2014, accepted in revised form 23rd November 2016)

Summary: At present hollow nanostructures have been intensive topics of research due to their superior properties over their solid nano counterparts. In this study uniform size chromium hollow nanospheres were synthesized by polyol method followed by simple corrosion etching using a proper solvent combination strategy. Fourier transform infrared (FTIR) and UV Visible spectroscopy have been applied to follow the conversion of precursor into metal particles and then hollow nanospheres respectively. Particle size and morphology have been characterized by particle size analyzer and Field Emission Scanning Electron microscopy (FE SEM). The crystal structures of chromium species such as CrO_2 and Cr_2O_3 resulted from CrOOH have been determined by X-ray diffraction technique (XRD). X-ray photoelectron spectroscopy (XPS) has been applied to evaluate the surface binding energy of chromium ions. Self arranged hollow nanospheres have shown temperature-dependent magnetization. In this way magnetic property of solid chromium nanospheres has been tuned by converting them into hollow nanospheres.

Key Words: Partially metallic chromium, Corrosion, Hollow nanospheres, Uniform size, Magnetic property.

Introduction

Hollow spheres with diameters ranging from nano to micro-scale dimensions have recently attracted special attention due to their unique properties such as low density, high specific surface, and large surface area with unusual mechanical/ thermal stability. Such structures have wide range of applications in catalysis, sorption, chemical & biological separations, coatings, drug delivery, cosmetics, inks, dyes and bio-medical electronic devices [1–7]. Now they have been utilized in energy related systems such as dye-sensitized solar cell, fuel cell, Li-ion batteries, super capacitors, etc [8, 9]. When used as fillers in preparing conductive composites, the hollow nanostructures also offer some advantages over their solid counterparts in terms of lighter weight, saving of material and reduction of cost. Moreover, Oldenburg et al. have reported the expanded spectral range of surface plasma resonance (SPR) of gold nanoshells from 600 nm to 1200 nm by varying their diameter and shell thickness [10, 11]. Methods to synthesize hollow materials include either template free or the use of various template precursors as reported elsewhere [6]. The later preparation often requires the removal of the template after synthesis utilizing separation techniques such as acid or base etching and calcinations [9, 12-16]. The development of simple, mild, and effective methods for creating hollow nanospheres is of importance to nanotechnology and remains a key research challenge.

As reported in literature, chromium metal and chromium oxide based compounds play an important role in the reduction of pollutants emitted from automobiles and serve as the primary catalysts for wide varieties of basic and industrial reactions such as polymerization (Philips catalysts), hydrogenation, dehydrogenation, oxidation, and isomerization reactions [17-25]. Chromium nanomaterials have improved the fluorescence of close proximity fluorophores up to eight times as reported recently [26]. Beside these, a great interest has been found in the ferro-magnetic chromium compounds, especially in half-metallic CrO_2 at room temperature because of its fully spin-polarized band structure at the Fermi level [27-29]. This makes CrO_2 a good candidate to be used as magnetic components in magneto electronic devices that require a large spin polarization such as magnetic tunnel junctions and spin valves [30-33]. Magnetic tapes prepared from CrO_2 are used for magnetic recording applications [34]. Now chromium oxide porous nano tubes have been applied as an ethanol sensor [35].

The performance of chromium based nanomaterials can be further tuned or improved for most of these applications through their nanostructures into hollow ones. Herein we report for the first time the synthesis of half metallic hollow chromium nanospheres and their characterization through sophisticated techniques.

Experimental

Materials

A.C.S. grade Tri-ethylene glycol, methanol, chloroform, polyvinylpyrrolidone (PVP) and Chromium acetate were purchased from Beijing

*To whom all correspondence should be addressed.

Chemical Reagent, Co. Ltd, China and used without further purification. The conversion of chromium acetate into chromium metal nanostructures was confirmed by Fourier-transform infrared (FTIR) spectroscopy. The spectra were obtained on Perkin Elmer Infrared Spectrometer using KBr disc in the range of 400–6000 cm^{-1}. UV/ Visible spectra of the solutions at different stages of the reaction were recorded by Jenway 6405 spectrophotometer. Particle size was measured by Particle Analyzer (Brookhaven Instrument Corp.) using 90 Plus Particle Sizing Software Ver.3.48. SEM images of hollow spheres were obtained by Field Emission Scanning Electron Microscope (JSM-6700F, JEOL, JAPAN). After precipitation, nanospheres were re-dispersed in equal volumes of methanol and chloroform. Then 5µl of this solution was drop cast on the surface of aluminum foil and allowed to dry in open atmosphere.

The crystalline structure of the samples was characterized by XRD on a D/MAX-RC diffractometer operated at 30 kV and 100 mA with Cu Kα radiation (λ = 1.5406 A°). The XPS measurement of the hollow nanospheres surface was performed on an ESCALab220i-XL spectrometer operated at 15 kV and 20 mA at a pressure of about 3×10−9 mbar using Al Kα as the exciting source (hv = 1486.6 eV). The binding energies were calibrated with respect to the signal for adventitious carbon (284.8 eV). The magnetic measurements were carried out in a SQUID magnetometer (MPMS) of Quantum Design. The zero-field cooled (ZFC) and field-cooled (FC) magnetization vs. temperature patterns was studied across a temperature range 2-390 K at the field 100 Oe.

Methods

Synthesis of chromium metal nanospheres

Chromium nanospheres were prepared by a modified polyols process as demonstrated in our previous work [36]. In experiment 1; a desired amount of PVP (5.00 M) was dissolved in reaction flask containing 60 ml of tri-ethylene glycol with constant stirring at 60 °C. Chromium acetate powder (0.814 M) was added and stirred by magnetic stirrer at 120 °C for 20 min to dissolve the solid chromium precursor as well as to remove any traces of water. The resulted mixture was refluxed under vigorous stirring at 285 °C. After 14 hrs a transparent dark brown homogeneous colloidal solution of Cr^0 nanoparticles was obtained without any precipitate. In experiment 2; other size nanostructures were obtained by the variation of molar ratio of PVP (4.0 M) to the same amount of chromium precursor and increasing the reflux time up to 20 hrs. Generally, as prepared polyol dispersion of Cr^0 structures was precipitated using anhydrous acetone. The precipitates were centrifuged, washed with acetone and re-dispersed in ethanol.

Conversion into partially metallic hollow nanospheres

Similarly two different size half metallic hollow spheres were prepared by the corrosion of above particles refluxing in a proper combination of ethanol, water, and chloroform .For example 48.3±1nm size chromium hollow nanospheres (Fig. 3) were obtained from first batch (named as Exp-1) after refluxing in ethanol, water and chloroform (4:3:3) for 20 hrs at 60 °C. Whereas second batch (named as Exp-2) chromium particles refluxed in same combination of solvents and reaction conditions, resulted 314.56±0.86 nm size hollow spheres (Fig. 4).

Results and Discussion

In this paper a very simple approach for the synthesis of half metallic chromium hollow nanospheres is being reported through etching process. First size controlled chromium metal nanoparticles was synthesized using modified polyol method [36], and then converted into very similar size and well-arranged hollow nanospheres. This conversion of chromium acetate into chromium metal nanostructures was confirmed by IR spectroscopy. In the spectrum of chromium metal nanostructures, the IR vibrational band due to Cr-O bond stretching of chromium acetate that appeared in the low zone at 661 cm^{-1} was completely disappeared [36-37] (Fig. 1).

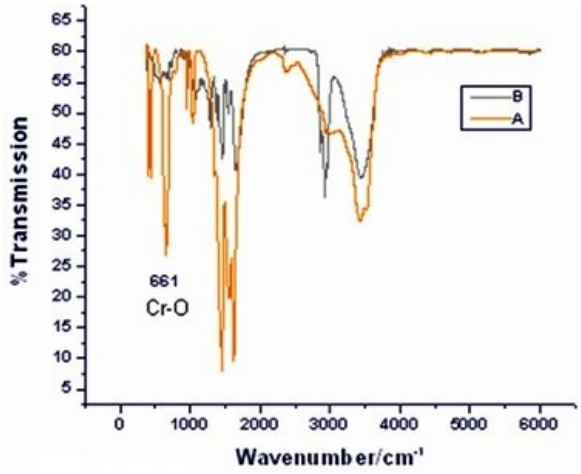

Fig. 1: FTIR spectra of Chromium Acetate (A) and Chromium Metal Nanomaterials (B).

To analyze the corrosive etching process that transformed Cr particles into hollow spheres,

UV/ Visible spectra of the solution were recorded at different stages of the reaction (Fig. 2). Change in the UV spectra within few hours indicated that the oxidative etching of the Cr clusters by air started at the early stages. The mixture of solvents such as water, ethanol, and chloroform dissolves the PVP from the surface of chromium particles. Chloride ions are generated by chemical activation of chloroform by electron transfer from nanoparticles to solvents and adsorbed on the nanoparticles surface [38, 39]. The peaks at 248 correspond to the complex formation of Cr to the ions of the chloroform within 5 hrs. While after 15 hrs the peaks at 298, 416 and 510-775 can be attributed to the water substituted chromium complexes. The concentration of water substituted chromium complexes increased with the passage of time as the particles were etched by corrosive pitting. Similarly for the corrosion of the bulk metal, O_2, Cl^- ions, and water all are the basic reasons for the initiation of the pitting at the surface of the chromium nanoparticles [16]. As reported in literature, corrosion commonly starts when the O_2 in air is dissolved in water on the surface of metal, picking up electron from the cathode to form hydroxide ions and then migrating towards the anode [38-40]. In this way the presence of chloroform and water plays a very important role in starting the corrosive etching by providing appropriate environment [38-40]. Therefore in the absence of either water or chloroform no hollow spheres were found.

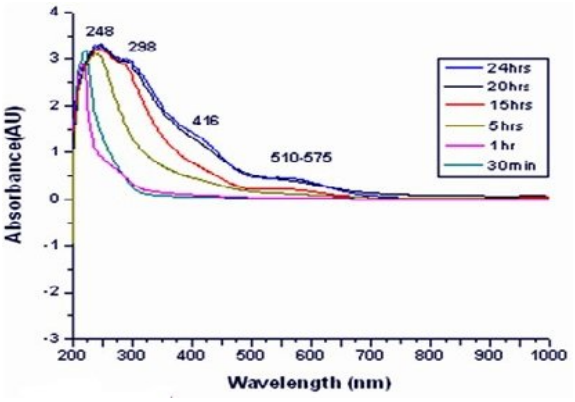

Fig. 2: UV Visible spectra showing different stages of oxidative etching during the conversion of chromium metal nanoparticles into hollow nanospheres

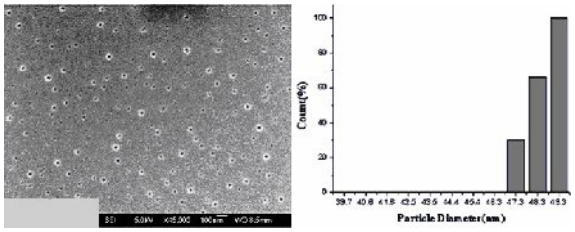

Fig. 3: Hollow nanospheres prepared at concentration of PVP(5.0M) & refluxing time 14 hrs. Brookhaven graph showing particle size 48.3±1nm.

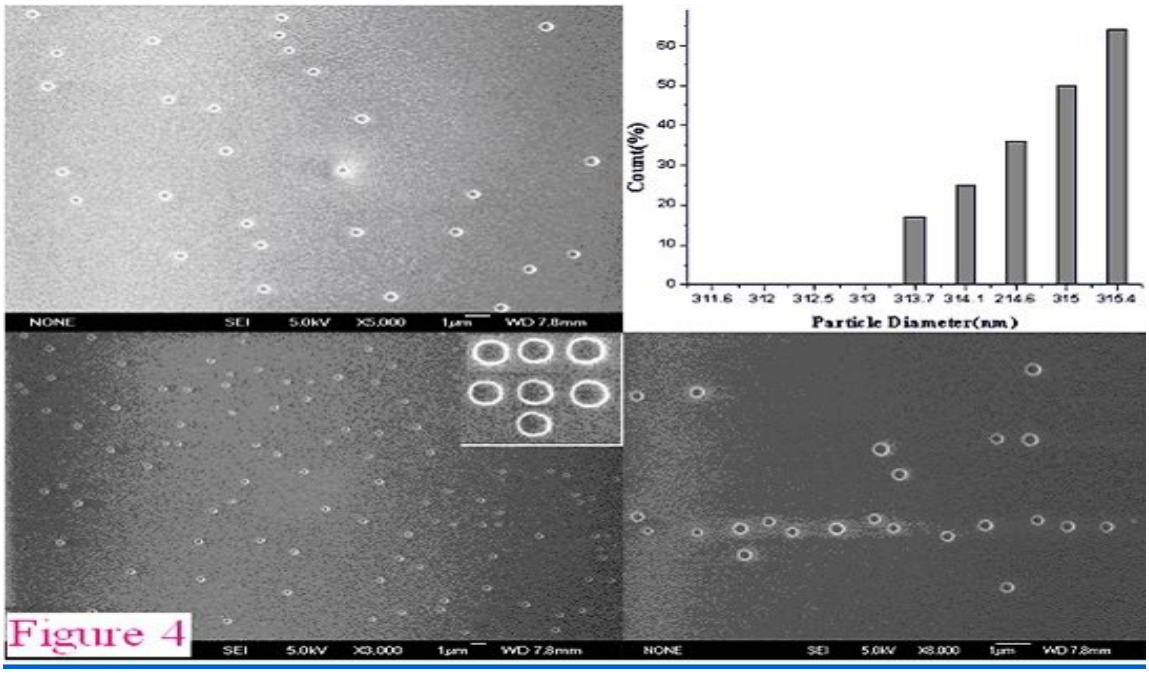

Fig. 4: Hollow nanospheres prepared at concentration of PVP(4.0M) & refluxing time 20 hrs. Brookhaven graph showing particle size 314.56±0.86nm and inset are enlarged hollow nanospheres.

The graph of particle size analyzer showed that the particles were well uniform in size and not agglomerated in clusters. It was observed that the concentration of PVP and the reaction time during the formation of metal particles play an important role in controlling the size of final nanospheres. For example in first experiment the concentration of PVP (5.0 M) and refluxing time 14 hrs generated 48.3±1nm chromium hollow spheres.

While in second experiment the decrease of concentration of PVP (4.0 M) and the enhanced reaction time up to 20 hrs resulted in 314.56±0.86nm size hollow spheres. The increase in diameter at low concentration of surfactant and the extended heating time is due to the intra or inter particle repining process as we have described earlier [36]. It was also noted that the hollow spheres were well arranged in chain forms perhaps due to their ferromagnetic property as reported in literature [41].

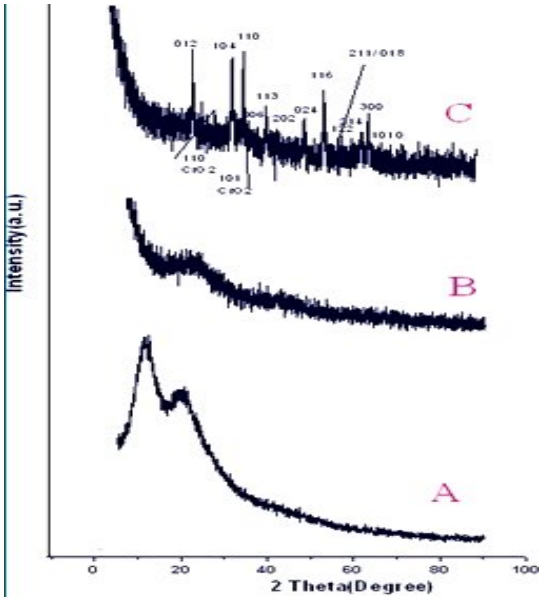

Fig. 5: XRD spectra of hollow nanospheres from Exp 1&2 calcined for 4hrs at 300 ^{o}C (A), calcined for 6 hrs at 450 ^{o}C, Exp-1 (B) and Exp -2 (C).

To evaluate the crystal structure of hollow nanospheres, both the materials were calcined at 300 ^{o}C for 4 hrs and subjected to powder XRD, which showed same pattern with no significant X-ray diffraction peaks indicating the materials are amorphous powder or poorly crystalline (Fig.-5A). Then materials were heated at 450 ^{o}C for 6 hrs and again XRD was carried out, but no typical peaks were observed for Exp-1 (Fig. 5B) which indicated that the material at this temperature is also in mixed phase of CrO_2 and CrOOH thermal transition species and the crystalline Cr_2O_3 is still at early stage. These transition species were either amorphous or in low concentration and could not be detected. While the X-ray diffraction pattern of nanomaterials from Exp-2 (Fig.-5C) showed a mixture of peaks for Cr_2O_3 resulted from CrOOH and CrO_2. After careful evaluation it was found that the diffraction pattern indexed to the rhombohedral structure as per literature JCPDS card Nos. 01-084-314 for Cr_2O_3 with poor peaks of CrO2. It is important to note that the rhombohedral Cr_2O_3 has the corundum type structure of space group R-3c with hexagonal close packed layers of oxygen atoms and two third of the octahedral holes in between filled by chromium atoms[42].

To further investigate the chemical composition of the hollow nanosphere surfaces, X-ray photoelectron spectroscopy (XPS) was performed, because spectral results from the interaction with chromium metal valence electrons can provide significant information about the metal ion. Chromium metal high resolution (Cr 2p) spectrum shows spin orbit splitting into Cr 2 $p_{1/2}$ and Cr $2p_{3/2}$ components and both contains similar qualitative information. Therefore here we are discussing only Cr $2p_{3/2}$ bands. The high resolution spectra of Cr $2p_{3/2}$ and O1s of the chromium hollow spheres are shown in Fig. 6A and 6B. The components of Cr $2p_{3/2}$ spread over 574- 578.7 eV and can be assigned to Cr^0 (574 eV), CrO_2 (576.3 eV), and Cr_2O_3 (576.8 eV) which are agreed in the literature values [31, 43, 44]; whereas higher side band up to 578.7 eV is attributed to CrOOH and H_2O species. Since the peak positions of above species are much closer so they are not separating to each other. All the components of O1s are in consistence with the values assigned to Cr 2p band. Here it is notable that Cr $2p_{3/2}$ band of Exp-1 is at higher energy side than that of Exp-2 indicating the presence of CrOOH in excess. While in Exp-2 oxides are dominated over CrOOH, which are completely in agreement with the results of XRD. The higher peak intensity for Cr_2O_3 than CrO_2 in Exp-2 is due to less stability of later species and readily conversion to chromium oxide at high temperature. Therefore the surface is almost covered by Cr_2O_3. As shown in the Fig. 6C, the peaks for N 1s in Exp- 2 band can be observed at 399.6 eV, which corresponds to the free nitrogen in five member ring of PVP, whereas the peak observed at 400.5 eV in the spectrum of Exp-1 can be attributed to the ionic nitrogen ($-N^{+}-$) species. This suggests that the chromium cations in Exp-1 still have interaction with the nitrogen of PVP. Due to the attraction of metal cation electrons move toward the metal causing the increase in binding energy of nitrogen to higher side as described elsewhere [45].

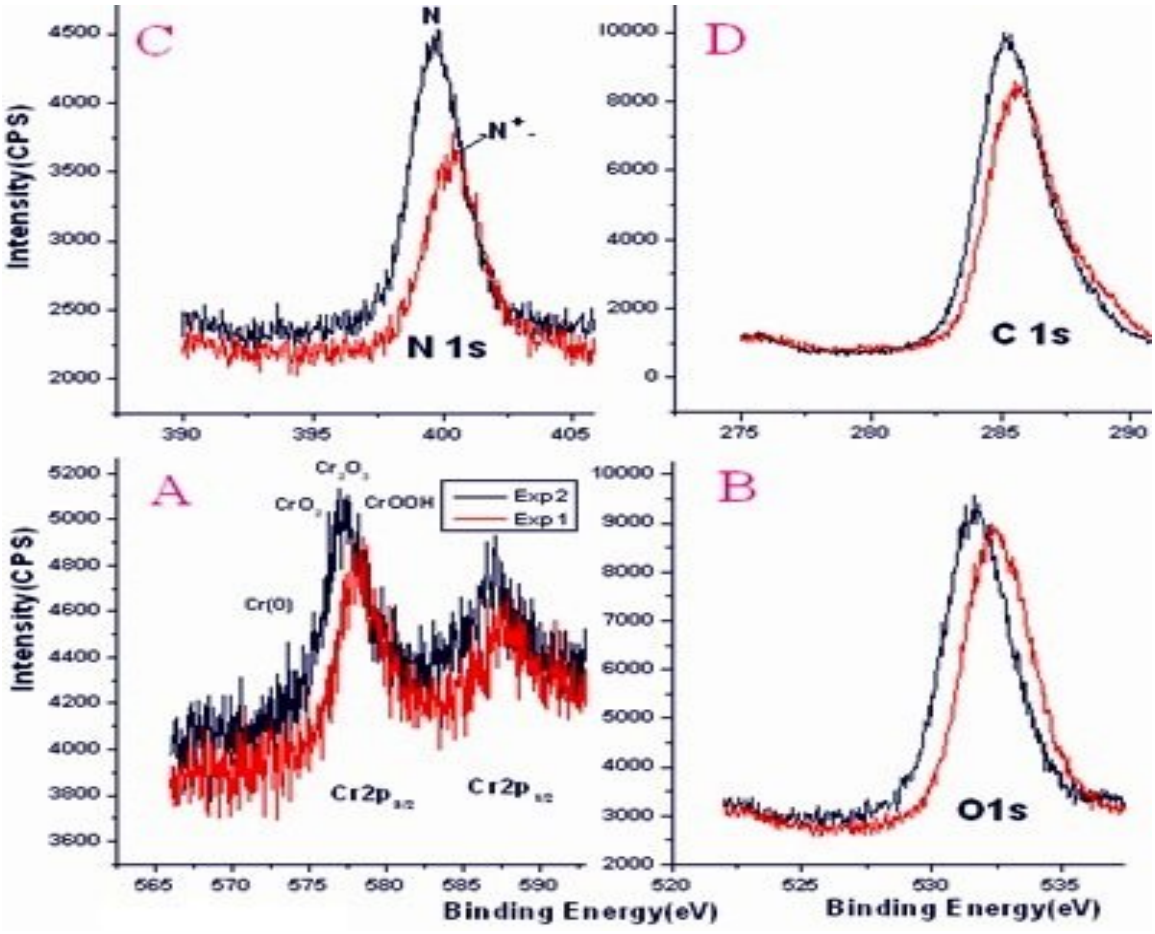

Fig. 6: XPS Spectra of hollow nanospheres for Cr 2p (A) ,O 1s (B) N 1s(C) and C 1s(D).

The self-alignment of hollow nanospheres was the indication of their magnetic property [41]. Therefore they were subjected to determine the temperature dependent-magnetization at 100 Oe field to collect the data from 2K-390K as shown in Fig. 7. It was noted that hollow nanospheres showed phase transitions at different temperature and reached the limit of equipment. Different factors for phase transition, such as particle size, influence of magnetic field, uniform pressure, first order transition in super conductors etc have been reported in literature [46-49]. But we believe that the phase transition here is due to the various thermal transition species of partially metallic hollow nanospheres, as discussed above in XRD and XPS results. Nanoporous materials composed of metal-assembled complexes may be expected to display some humidity response because materials in this category can show functionalities such as gas storage and molecular recognition [50-51]. However a detailed study in future will reveal the actual reason of such behavior of hollow nanospheres.

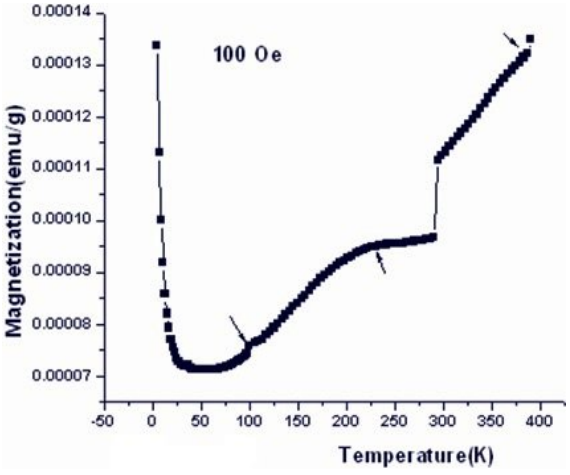

Fig. 7: The temperature-dependent magnetization curve of partially metallic chromium hollow nanospheres (48.3±1nm) at 100 Oe

Conclusions

It is concluded that the successful preparation of chromium metal nanomaterials by polyols method and then their conversion into partially metallic hollow nanospheres using solvent combination is very simple and feasible approach. Chloroform and water are the essential parts to start the corrosion process on the surface of metal nanoparticles. The size of hollow nanospheres depends upon the size of metal nanoparticles that can be increased or decreased by changing the amount of PVP and reaction time. Hollow nanospheres are monodispersed but well aligned as shown in SEM images. Cr (0), CrO_2, CrOOH, and Cr_2O_3 are the major components of hollow nanospheres as revealed by the XRD and XPS. At last, hollow nanospheres have tuned magnetic property of their solid counterparts. Therefore we hope that chromium hollow nanospheres may improve other properties such as catalytic activities.

Acknowledgments

We are very thankful to the Third World Academy of Sciences (TWAS), Chinese Academy of Sciences (CAS) for providing Postdoctoral fellowship to conduct this work in China.

References

1. Y. Yin, R. M. Rioux, C. K. Erdonmez, S. Hughes, G. A. Somorjai and A. P. Alivisatos, Nanocrystals Through the Nanoscale Kirkendall Effect, *Science*, **304,** 711 (2004).
2. A. B. Bourlinos, M. A. Karakassides and D. Petridis, Synthesis and Characterization of Hollow Clay Microspheres through a Resin Template Approach**,** *Chem. Commun.,* **16**, 1518 (2001).
3. D. Zhang, L. Qi, J. Ma and H. Cheng, Synthesis of Submicrometer-Sized Hollow Silver Spheres in Mixed Polymer-Surfactant Solutions**,** *J. Adv. Mater.*, **14,** 1499 (2002).
4. G. R. Yi, S. J Jeon, T. Thorsen, V. N. Manoharan, S. R. Quake, D. J. Pine and S. M. Yang, Generation of Uniform Photonicballs by Template-Assisted Colloidal Crystallization, *Synthetic Metals*, **139,** 036 (2003).
5. K. An, and T. Hyeon**,** Synthesis and Biomedical Applications of Hollow Nanostructures**,** *Nano Today,* **4,** 359 (2009).
6 J. Hu, M. Chen, X. Fanga and L. Wu, Fabrication and Application of Inorganic Hollow Spheres**,** *Chem. Soc. Rev.,* **40,** 5472 (2011).
6. G. Maccauro, P. R. Iommetti, F. Muratori, L. Raffaelli, P. F. Manicone and C. Fabbriciani, An Overview about Biomedical Applications of Micron and Nano Size Tantalum**,** *Recent Patents on Biotechnology*, **3,** 157 (2009).
7. G. Maccauro, P. R. Iommetti, F. Muratori, L. Raffaelli, P.F. Manicone and C. Fabbriciani, An Overview about Biomedical Applications of Micron and Nano Size Tantalum**,** *Recent Patents on Biotechnology*, **3,** 157 (2009).
8. J. Liu and D. Xue, Hollow Nanostructured Anode Materials for Li-Ion Batteries**,** *Nanoscale Res. Lett*, **5,** 1525 (2010).
9. X. Lai, J. E. Halpert and D. Wan, Recent Advances in Micro-/Nano-Structured Hollow Spheres for Energy Applications: From Simple to Complex Systems, *Energy Environ. Sci.,* **5,** 5604 (2012).
10. M. Ohmori and E. Matijevic, Preparation and Properties of Uniform Coated Colloidal Particles. VII. Silica on Hematite**,** *J. Colloid. Interface Sci.*, **150,** 594 (1992).
11. S. J. Oldenburg, R. D. Averitt, S. L. Westcott and N. J.Halas, Nano-Engineering of Optical Resonances, *Chem. Phys. Lett.*, **288,** 243 (1998).
12. S. Han, K. Sohn and T. Hyeon, Fabrication of New Nanoporous Carbons through Silica Templates and their Application to the Adsorption of Bulky Dyes, *Chem. Mater.*, **12,** 3337 (2000).
13. S. W. Kim, M. Kim, W. Y. Lee and T. Hyeon, Fabrication of Hollow Palladium Spheres and their Successful Application to the Recyclable Heterogeneous Catalyst for Suzuki Coupling Reactions, *J. Am. Chem. Soc.*, **124,** 7642 (2002).
14. J. Lee, K. Sohn and T. Hyeon**,** Fabrication of Novel Mesocellular Carbon Foams with Uniform Ultralarge Mesopores, *J. Am. Chem. Soc.*, **123,** 5146 (2001).
15. T. Liu, Q. Wan, Y. Xie, C. Burger, L. Liu and B. Chu**,** Polymer-Assisted Formation of Giant Polyoxomolybdate Structures, *J. Am. Chem. Soc.*, **123,** 10966 (2001).
16. D. Nagao, C. M. V. Kats, K. Hayasaka, M. Sugimoto, M. Konno, A. Imhof and A. V. Blaaderen**,** Synthesis of Hollow Asymmetrical Silica Dumbbells with a Movable Inner Core**,** *Langmuir*, **26,** 5208 (2010).
17. A. K. Sinha and K. Suzuki, Three-Dimensional Mesoporous Chromium Oxide: A Highly Efficient Material for the Elimination of Volatile Organic Compounds**,** *Angew. Chem. Int. Ed.*, **44**, 271 (2004).
18. N. D. Hahn, M. N. Nieger and K. N. Dotz**,** Highly Regio- and Diastereoselective Chromium(0) -Catalysed Cyclopropanation of 1-

Alkoxy-1,3-dienes with Diazo Compounds, *Eur. J. Org. Chem.*, **2004**, 1049 (2004).
19. D. Mohring, M. Nieger, B. Lewall and K. H. Dotz, Tricarbonyl (naphthoquinone) Chromium: Synthesis and Application in [4+2] Cycloaddition Reactions, *Eur. J. Org. Chem*, **2005,** 2620 (2005).
20. J. H. Rigby, M. A. Kondratenko and C. Fiedler, Preparation of a Resin-Based Chromium Catalyst for Effecting [6pi + 2pi] Cycloadditions of Allenes, *Org. Lett.*, **2,** 3917 (2000).
21. J. P. Hogan, Ethylene Polymerization Catalysis over Chromium Oxide, *J. Polym. Sci.,* **8,** 2637 (1970).
22. G. Mani and F. P. Gabba, A Neutral Chromium(iii) Catalyst for the Living "Aufbaureaktion", *Angew. Chem. Int. Ed.*, **43,** 2263 (2004).
23. S. Wang, K. Murata, T. Hayakawa, S. Hamakawa and K. Suzuki, Dehydrogenation of Ethane with Carbon Dioxide over Supported Chromium Oxide Catalysts, *Appl. Catal. A.*, **19,** 1 (2000).
24. L. M. Madeiraa and M. F. Portelab, Catalytic Oxidative Dehydrogenation of *n*-butane, *Cata.l Rev: Science and Engineering*, **44,** 247 (2002).
25. X. Zhao and X. Wang. Oxidative Dehydrogenation of Ethane to Ethylene by Carbon Dioxide Over Cr/TS-1 Catalysts, *Cata.l Comm.*, **7**, 633 (2006).
26. R. Pribik, K. Aslan, Y. Zhang and C. D. Geddes, Metal-Enhanced Fluorescence from Chromium Nanodeposits, *J. Phys. Chem. C.*, **112,** 17969 (2008).
27. K. Inoue, K. Kikuchi, M. Ohba and H. Okawa, Cover Picture:Structure and Magnetic Properties of a Chiral Two-Dimensional Ferrimagnet with TC of 38 K, *Angew. Chem. Int. Ed.*, **42,** 4810 (2003).
28. D. M. Low, G. Rajaraman, M. Helliwell, G. Timco, J. van Slageren, R. Sessoli, S. T. Ochsenbein, R. Bircher, C. Dobe, O. Waldmann, H. U. Güdel, M. A. Adams, E. Ruiz, S. Alvarez, E. J. L. McInnes, Family of Ferro- and Antiferro-magnetically Coupled Decametallic Chromium(III) Wheels *, Chem.A Eur. J.,* **12**, 1385 (2006).
29. M. R. Fitzsimmons, J. A. Eastman, R. A. Robinson and J. W. Lynn, On the Possibility of a Two-State Magnetic Structure for Nanocrystalline Chromium, *Nanostructured Mat.*, **7,** 179 (1996).
30. J. Dijkstrat, H. H. Weitering, C. F. van Bruggen, C. Haast and R. A. de Groot, Band-Structure Calculations, and Magnetic and Transport Properties of Ferromagnetic Chromium Tellurides, *J. Phys. Condens. Matter.*, **1,** 9141 (1989).
31. Y. Chen, K. Ding, L. Yang, B. Xie, F. Song, J. Wan, G. Wang and M. Hana, Nanoscale Ferromagnetic Chromium Oxide Film Gas-Phase Nanoclusters Deposition, *App.l Phys. Lett.*, **92,** 173112 (2008).
32. J. Y. Son and J. H. Cho, Characterization of Half-Metallic CrO_2-Coated Cantilevers, *Nanotechnology*, **18,** 165503 (2007).
33. Y. Song, A. L. Schmitt and S. Jin, Spin-Dependent Tunneling Transport into CrO_2 Nanorod Devices with Nonmagnetic Contacts, *Nano Lett.*, **8,** 2356 (2008).
34. J. P. Dismukes, D. F. Martin, L. Ekstrom, C. C. Wang and M. D Coutts, Ferromagnetic Chromium Dioxide for Magnetic Tape, *Ind. Eng. Chem. Prod. Res. Develop.*, **10,** 319 (1971).
35. G. An, Y. Zhang, Y. Z. Liu, Z. Miao, B. Han, S. Miao and J. Li, Preparation of Porous Chromium Oxide Nanotubes Using Carbon Nanotubes as Templates and their Application as an Ethanol Sensor, *Nanotechnology*, **19,** 35504 (2008).
36. H. R. Nawaz, and Y. Zhang, Size-Controlled Synthesis of Chromium Nanosheres and Conversion into Multipods, Rods, Rectangular Blocks, Complex Structures and Superlattice Self-Assemblies, *J. Chem. Soc. Pak.*, **31,** 240 (2009).
37. R. Swaminathan, In *NE226 L Characterization of Materials Experiment Fourier Transform Infrared Spectroscopy*, p.4 (2007).
38. S. J. Lim, W. Kim, S. Jung, J. Seo and S. K. Shin, Anisotropic Etching of Semiconductor Nanocrystals *Chem. Mater.*, **23,** 5029 (2011).
39. I. H. Ling, Room-Temperature Formation of Hollow Cu_2O Nanoparticles, *Advanced Materials*, **22,** 1910 (2010).
40. Y. Xiong, B. Wiley, J. Chen, Z.Y. Li, Y. Yin and Y. Xia, Corrosion-Based Synthesis of Single-Crystal Pd Nanoboxes and Nanocages and their Surface Plasmon Properties*, Angew. Chem. Int. Ed.*, **44,** 7913 (2005).
41. H. Wang, Y. Yu, Y. Sun and Q. Chen, Magnetic Nanochains: A Review, *NANO: Brief Reports and Reviews*, **6,** 1 (2011).
42. M. Catti, G. Sandrone, G. Valerio and R. Dovesi, Electronic, Magnetic and Crystal Structure of Cr_2O_3 by Theoretical Methods, *J. Phys. Chem. Solids.*, **57,** 1735 (1996).
43. R. Cheng, C. N. Borca, N. Pilet, B. Xu, L. Yuan, B. Doudin, S. H. Liou and P. A. Dowben, Oxidation of Metals at the Chromium Oxide Interface, *Appl Phys. Lett.*, **81,** 2109 (2002).
44. R. Cheng, B. Xu, C. N. Borca, A .Sokolov, C. S. Yang, L. Yuan, S. H. Liou, B. Doudin and P. A.

Dowben, Characterization of the Native Cr_2O_3 Oxide Surface of CrO_2**,** *Appl Phys. Lett*., **79,** 3122 (2001).

45. C. K. I. Tan, K. Yao, P. C. Goh and J. Ma, 0.94(K0.5Na0.5)NbO3–0.06LiNbO3 Piezoelectric Ceramics Prepared from the Solid State Reaction Modified with Polyvinylpyrrolidone (PVP) of Different Molecular Weights, *Ceramics International*, **38,** 2513 (2012).
46. R. Mazumder, S. Ghosh, P. Mondal, D. Bhattacharya, S. Dasgupta, N. Das, A. Sen, A. K. Tyagi, M. Sivakumar, T. Takami and H. Ikuta, Particle Size Dependence of Magnetization and Phase Transition Near TN in Multiferroic $BiFeO_3$, *J. Appl. Phys.*, **100,** 33908 (2006).
47. K. Y. Mulyukov and I. I**.** Musabirov, Influence of Magnetic Field Intensity on the Temperature Dependence of Magnetization of Ni2.08Mn0.96Ga0.96 Alloy, *JEEMA***, 2,** 431 (2010).
48. S. A. Nikitin and R. V. Bezdushnyi**,** Uniform Pressure Effect on Magnetic Phase Transitions and Magnetization of Single Crystals of TbxY1−x Alloys *physica. Status. Solidi*, **124,** 327 (1991).
49. S. B. Roy, M. K. Chattopadhyay and P. Chaddah**,** Temperature Dependence of Magnetization in the Superconducting Mixed State of $CeRu_2$: Evidence of a First-Order Phase Transition, *J. Phys: Condensed Matter*, **18,** 9471 (2006).
50. S. Ohkoshi, K. Arai1, Y. Sato and K. Hashimoto, Humidity-Induced Magnetization and Magnetic Pole Inversion in a Cyano-Bridged Metal Assembly*, Nature Materials*, **3,** 857 (2004).
51. Z. Lu, X. Wang, Z. Liu, F. Liao, S. Gao, R. Xiong, H. Ma, D. Zhang and D. Zhu, Tuning the Magnetic Behavior via Dehydration/Hydration Treatment of a New Ferrimagnet with the Composition of K0.2Mn1.4Cr(CN)6â6H2O, *Inorg. Chem.*, **45,** 999 (2006).